Preprints.org

Article

Design and Performance of High-Capacity Magnesium-Air Battery for Power Generator System

Kwang-Yeop Jang , Sang-Won Seo , Dong-Jin Kim [*] , Dong-Gun Lee [*]

Article

Design and Performance of High-Capacity Magnesium-Air Battery for Power Generator System

Kwang-Yeop Jang [1,2], Sang-Won Seo [3], Dong-Jin Kim [3,*] and Dong-Gun Lee [2,4,*]

[1] Korean Testing Certification Institute, Reliability & Semiconductor Convergence Center, Gunpo 15809, Republic of Korea
[2] Tech University of Korea, Graduate school, Electrical Engineering, Siheung 15073, Republic of Korea
[3] SUNKWANG LTI, Research & Development, Seoul 06230, Republic of Korea
[4] Tech University of Korea, Department of Energy & Electrical Engineering, Siheung 15073, Republic of Korea
[*] Correspondence: rnd@i-sk.com (D.-J.K.); dglee@tukorea.ac.kr (D.-G.L.)

Abstract: Efforts to achieve carbon neutrality, which aims to reduce the net carbon emissions to zero by decreasing carbon emissions from human activities and increasing carbon absorption, are actively underway. Additionally, the search for clean energy alternatives to fossil fuels has become a global research trend. This paper presents research on metal-air batteries, focusing on the development of energy supply technologies that do not generate carbon emissions during power generation and require less space for power generation compared to existing renewable energy sources. The proposed Mg-Air Battery (MAB) in this study uses magnesium as the metal anode and theoretically offers a maximum open-circuit voltage of 3.1V and a high energy density of 6.8kWh/kg. While previous research has primarily focused on designing small-capacity cells and maximizing the performance of metal anodes, this study differentiates itself by designing a large-capacity MAB cell and optimizing its electrical performance. For the large-capacity cell design, the weight, shape, and size of the anode were designed based on MAB performance factors, and research was conducted on manufacturing methods to optimize the performance of the air cathode. Furthermore, to enhance usability and extend the lifespan of the MAB cell, it was designed to allow electrolyte circulation, and the electrolyte circulation performance was verified through simulations of fluid flow within the cell. Based on the study of the power performance of the newly designed large-capacity MAB cell, the feasibility of constructing a kW-class system using multiple Mg-Air battery cell stacks was confirmed.

Keywords: Magnesium-Air Battery (MAB); metal-air battery cell design; electrical performance; eco-friendly distributed power supply

1. Introduction

The widespread industrialization and the use of fossil energy sources have led to the emission of significant amounts of greenhouse gases, which in turn have caused global warming, environmental changes, and continuous environmental problems [1]. Since pre-industrial times in around 1850, the average global atmospheric concentration of carbon dioxide (CO_2) has risen from 285 ppm to 419 ppm by 2022 [2]. According to the UK Met Office, the global average surface temperature has increased by approximately 0.97 to 1.21°C during the period of 1850 to 2022, with an estimated increase of about 1.09°C. It is anticipated that global greenhouse gas emissions will increase by 50% by 2050, primarily due to CO_2 emissions from the use of non-renewable energy sources. Without effective measures or technologies to reduce or control CO_2 emissions, both the global average atmospheric CO_2 concentration and the temperature of the Earth's surface and oceans will continue to rise. The temperature rise caused by greenhouse gases is already expected to cause major damage to human living environments, such as the extinction of some species, loss of biodiversity, droughts, floods, wildfires, ocean acidification, the melting of the North and South Polar Glaciers (NSPG), and sea level rise, making it urgent to implement countermeasures [3–5].

The metal-air battery is a type of electrochemical cell that operates through the oxidation of metal and the reduction of oxygen. It features an energy density that is 3 to 30 times higher than the widely used Lithium-Ion Battery (LIB) [6]. Additionally, metal-air batteries have the advantages of relatively low explosion risk and being environmentally friendly energy storage devices.

The components of a metal-air battery consist of a porous air cathode for the continuous supply of oxygen, a metal anode, an electrolyte that separates the two electrodes, and the cell frame. Metals used as the metal anode in metal-air batteries include Li, Na, Fe, Zn, Al, and K, among others. Various elements with excellent electrochemical oxidation reactivity can be utilized as metal anode materials. Additionally, available electrolytes include aqueous electrolytes, non-aqueous electrolytes, hybrid electrolytes, and solid electrolytes.

Figure 1 shows a schematic diagram of the operation of a metal-air battery and illustrates the oxidation reaction process during operation. The metal-air battery is a type of energy storage device that utilizes the redox (reduction-oxidation) reaction, where metal ions transfer from the anode to the cathode, similar to ion batteries. The charge and discharge characteristics of a metal-air battery involve the metal anode losing electrons and transforming into metal ions, which dissolve in the electrolyte during discharge. At the cathode, the electrolyte (H_2O) and oxygen react to form OH^- (hydroxyl ions). For instance, magnesium (Mg) at the anode oxidizes to Mg^{2+}, releasing two electrons, and Mg^{2+} reacts with OH^- to form $Mg(OH)_2$.
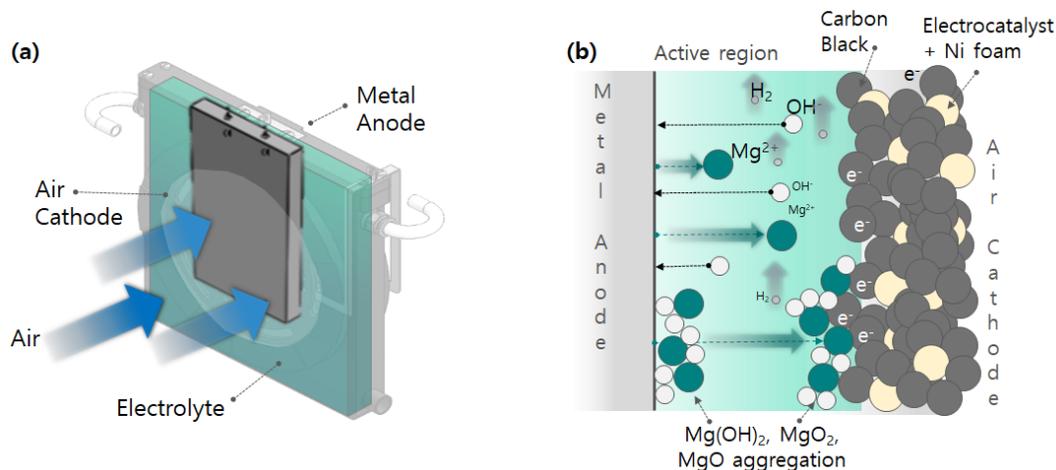
Figure 1. Schematic diagram of the operation of metal-air battery power generation. (a) Metal-Air Battery operation, (b) Metal-air battery oxidation reaction process.

The reaction equations for metal-air batteries vary depending on the choice of electrolyte and metal, as these factors influence the potential difference due to the movement of electrons. The general reaction in a metal-air battery can be described as follows:

$$\text{Metal Anode: } M \leftrightarrow M^{n+} + ne^- \tag{1}$$

$$\text{Air Cathode: } O_2 + ne^- + 2H_2O \leftrightarrow 4OH^- \tag{2}$$
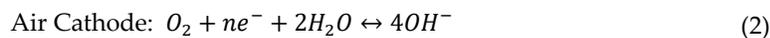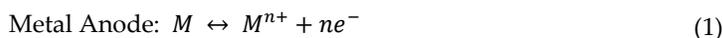
The metal-air battery generates electrical energy through oxidation reactions involving non-ferrous metals and a porous air cathode. Metal-air batteries have garnered significant interest in fields such as energy storage systems and mobility due to their theoretically high volumetric energy density, low material costs, and the potential for sustainable energy storage through the replacement of consumable materials. Among various power generation and energy storage technologies, the metal-air battery, which utilizes the reaction between non-ferrous metals and oxygen (O_2), has attracted attention from many researchers because of its high theoretical energy density and zero carbon emissions [7,8].

Metal-air batteries can utilize various metals such as lithium (Li), zinc (Zn), magnesium (Mg), and aluminum (Al), with oxygen from the air serving as one of the primary reactants. Recently, due to safety concerns associated with Li-battery fires and rising material costs, metal-air batteries have gained attention as a safer, more cost-effective, and environmentally friendly alternative. Metal-air batteries are considered a potential substitute for lithium-ion batteries due to their environmental friendliness, the abundance of resources, and high energy density, which meet the growing demand for energy storage technologies. Consequently, active research on various metal-air battery technologies is ongoing.
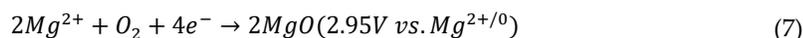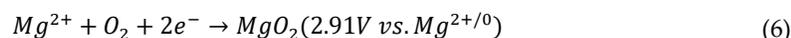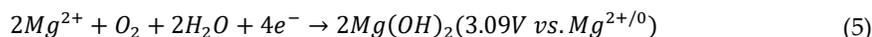
The Mg-Air Battery(MAB) theoretically exhibits a maximum voltage of 3.1V. One of the advantages of using magnesium in a metal-air battery is that magnesium is abundantly available and evenly distributed across the Earth. Additionally, magnesium offers excellent energy storage potential, fast electrochemical reaction kinetics, and due to its non-toxic and lightweight nature, it is easy to handle.

The energy generation process in a mg-air battery involves the oxidation of magnesium at the anode, where Mg^{2+} ions are produced, releasing two electrons. Oxygen (O_2) moves through the air cathode and interacts with water (H_2O) to form hydroxide ions (OH^-), facilitating electron transfer and generating electrical energy. The theoretical reactions for the mg-air battery are as follows:

$$Mg \rightarrow Mg^{2+} + 2e^- \tag{3}$$
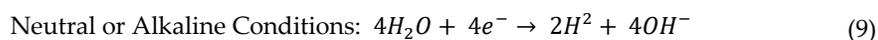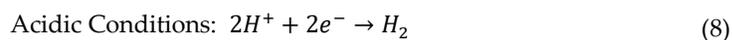
$$Mg^{2+} + 2OH^- \rightarrow Mg(OH)_2 + 2e^- \tag{4}$$
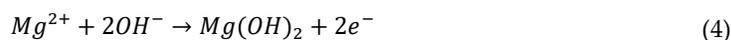
In this process, the Mg^{2+} ions generated at the anode combine with hydroxide ions produced at the cathode to form magnesium hydroxide ($Mg(OH)_2$), the main discharge product. In some cases, depending on the specific electrolyte used, discharge products such as magnesium oxide (MgO) or magnesium peroxide (MgO_2) can also be formed.

In the case of the mg-air battery, the oxygen molecules from the air, combined with electrons and water molecules, are reduced to hydroxide ions. These hydroxide ions further react with the Mg^{2+} ions generated from the metal anode, forming magnesium hydroxide, as described in the following reaction [9,10]:

$$2Mg^{2+} + O_2 + 2H_2O + 4e^- \rightarrow 2Mg(OH)_2 (3.09V \; vs. \, Mg^{2+/0}) \tag{5}$$

$$Mg^{2+} + O_2 + 2e^- \rightarrow MgO_2 (2.91V \; vs. \, Mg^{2+/0}) \tag{6}$$

$$2Mg^{2+} + O_2 + 4e^- \rightarrow 2MgO (2.95V \; vs. \, Mg^{2+/0}) \tag{7}$$

During discharge, the reaction product in this non-protonic electrolyte is magnesium hydroxide. In certain conditions, the discharge products may also include magnesium oxide and/or magnesium peroxide, depending on the specific electrolyte and reaction environment. These discharge products are formed as the battery completes its energy generation cycle.

Currently, for Mg-Air Battery(MAB) to be widely adopted as energy storage devices, there are several research challenges that need to be addressed. One of the key issues is reducing the corrosion rate of the metal caused by the Hydrogen Evolution Reaction (HER), which can occur under different conditions:

$$\text{Acidic Conditions: } 2H^+ + 2e^- \rightarrow H_2 \tag{8}$$

$$\text{Neutral or Alkaline Conditions: } 4H_2O + 4e^- \rightarrow 2H^2 + 4OH^- \tag{9}$$

In addition to managing corrosion, it is important to increase the discharge voltage to enhance the usable capacity. However, raising the discharge voltage accelerates the reaction between magnesium and oxygen, leading to increased byproduct formation during discharge and higher electrolyte consumption, which shortens the operating time per cell.

During the discharge process of MAB, byproducts such as magnesium hydroxide ($Mg(OH)_2$), magnesium oxide (MgO), and magnesium peroxide (MgO_2) are generated. These byproducts, often referred to as "slurry," do not decompose within the voltage range and tend to remain in the electrolyte or precipitate inside the cell, forming layers. The accumulation of byproducts slows down the metal-air battery's durability and corrosion reaction, eventually limiting its performance.

However, research on MAB is ongoing, with efforts focused on improving performance through the development of electrolyte circulation systems and surface treatment methods for metal anodes. These advancements aim to reduce the adverse effects of byproduct formation and enhance the overall durability and efficiency of MAB [11–15].

2. Mg-Air Battery Cell Design

2.1 Mg Anode Alloy Selection

An experiment was conducted to select the optimal Mg alloy material for the metal anode to achieve the best performance. To identify the most suitable metal anode based on magnesium, the electrical performance of five different Mg alloys (Pure Mg, LZ41, AL41, ZK60, and AZ31 in Figure 2) was compared. The reason for using Mg alloys as metal anodes is that alloying magnesium can refine the metal's microstructure, thereby enhancing its strength and corrosion resistance [16–27].

For the optimization of the Mg alloy metal anode, samples with identical dimensions (120mm x 100mm x 4T) were prepared. The experiments were conducted in an electrolyte solution of NaCl (18 wt%), with a 2.5mm gap between the metal anode and the air cathode. Discharge tests were carried out using a battery tester (WBCS3000S/WonATech) at currents ranging from 1.5A to 3.0A.

Figure 3 shows a graph comparing the voltage performance of various Mg alloys. The experimental results for the MAB cell's voltage performance indicated that magnesium-aluminum-based alloys outperformed other metal alloys in terms of voltage output. Among them, AZ31 (composed of Mg-96%, Al-3% and Zn-1%) exhibited the best electrical performance and was ultimately selected as the optimal material.

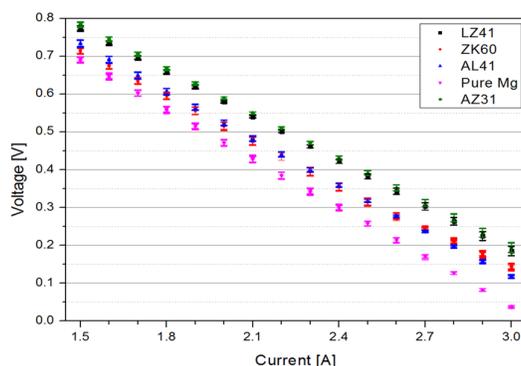**Figure 2.** Magnesium alloy anode sample.

Figure 3. Comparison on voltage performance of various magnesium alloy composition.

The reason for using alloyed Mg instead of pure Mg in metal-air batteries is that it enhances the electrochemical activity of the anode without significantly compromising the corrosion resistance during discharge. In particular, AZ (Al, Zn alloy) series alloys have been known since 1969 for their excellent mechanical properties and relatively superior corrosion resistance. The small amount of zinc (Zn) in these alloys helps reduce the self-corrosion rate during metal-air battery discharge, which improves electrochemical performance [28–30].

Among the AZ series, AZ31 and AZ91 exhibit high electrochemical reactivity as metal-air battery anodes. They are also widely available and easy to use due to their large-scale production, driven by high demand for Mg alloys, which keeps costs low. Additionally, compared to other alloy materials, AZ31 and AZ91 offer excellent corrosion resistance during discharge and produce fewer byproducts, making them advantageous for use in metal-air batteries.

2.2. Effect of Mg Anode-Air Cathode Gap Distance

As shown in Figure 4, the gap distance (d) between the metal anode and the air cathode plays a crucial role in the electrical performance of metal-air batteries. This is because, during operation, external air penetrates the porous air cathode and reacts with the metal anode inside the cell. When the gap distance is small, the movement of electrons is more efficient and faster, leading to improved power performance. However, if the distance is too large, the electron transfer is delayed, resulting in reduced electrical performance.
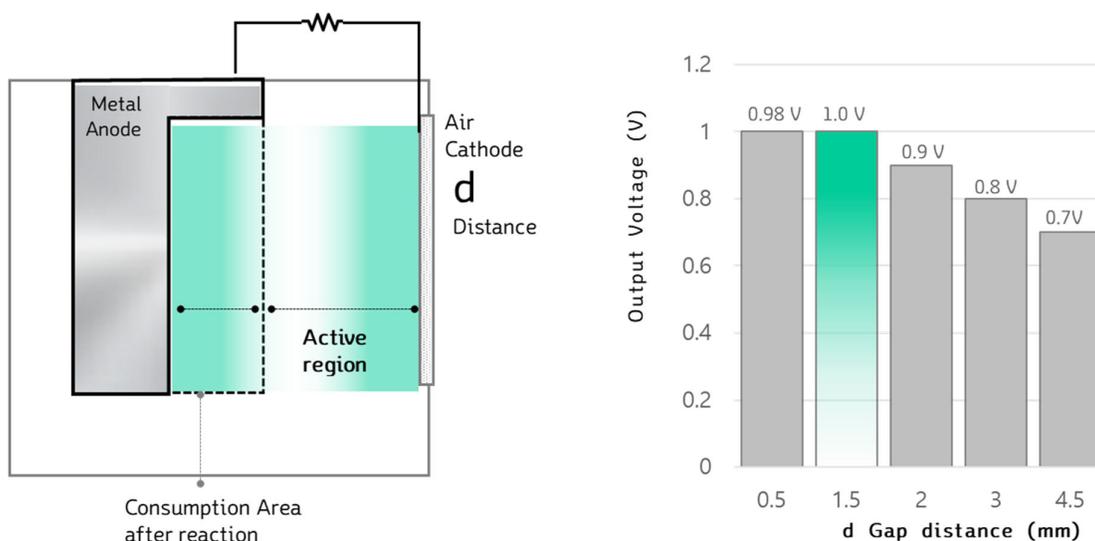

Figure 4. Schematic diagram on gap distance experiment of Mg-Air Battery.

On the other hand, if the gap distance is too small, it can cause damage to the air cathode or lead to excessive accumulation of by-products (such as $Mg(OH)_2$, MgO, or MgO_2) between the metal anode and the air cathode. These by-products may stack up excessively within the cell, negatively affecting its lifespan. Additionally, the electrochemical reactions generate heat, which can raise the cell temperature, potentially causing electrolyte evaporation.

Therefore, to optimize the design of the Mg-Air Generator(MAG) system, it is essential to determine the optimal gap distance. This distance should balance power performance and prevent excessive by-product accumulation or damage to the air cathode. Further research is needed to identify the gap distance that maximizes electrical performance without compromising the longevity and efficiency of the cell.

Figure 5 presents a graph comparing the voltage performance of a single MAB (metal-air battery) cell based on changes in the gap distance between the metal anode and the air cathode. The setup for the metal-air battery cell consisted of a 120 x 100mm, 4t Mg metal anode, and an electrolyte solution

(NaCl, 15~20wt%). Voltage performance was measured as the distance between the electrodes varied from 0.5mm to 4.5mm. To determine maximum performance, the discharge current was set to 5A using a battery tester (WBCS3000S/ WonATech).
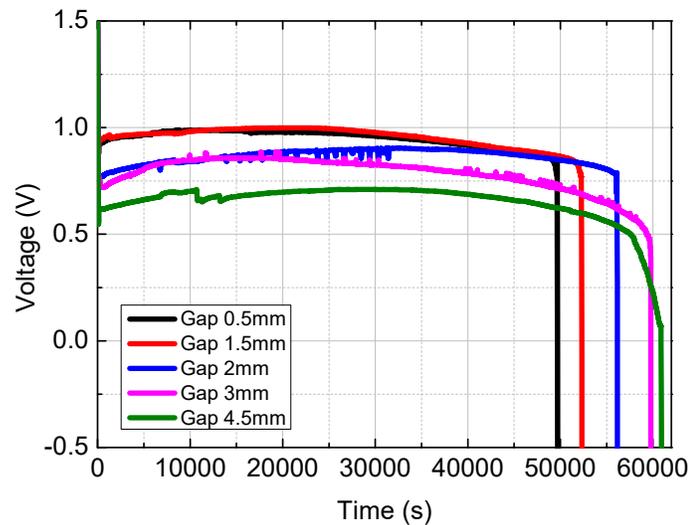
Figure 5. Comparison on voltage output according to change in gap distance of Mg-Air Battery.

The results showed that the highest voltage output, approximately 1.0V, occurred when the gap distance was between 0.5mm and 1.5mm, where the metal anode was closest to the air cathode. In contrast, the voltage performance decreased significantly as the distance increased, with the lowest voltage output of 0.70V observed at a 4.5mm gap distance. This indicates that the closer the gap distance, the higher the voltage performance, although an optimal balance must be struck to avoid excessive by-product accumulation and potential cell damage.
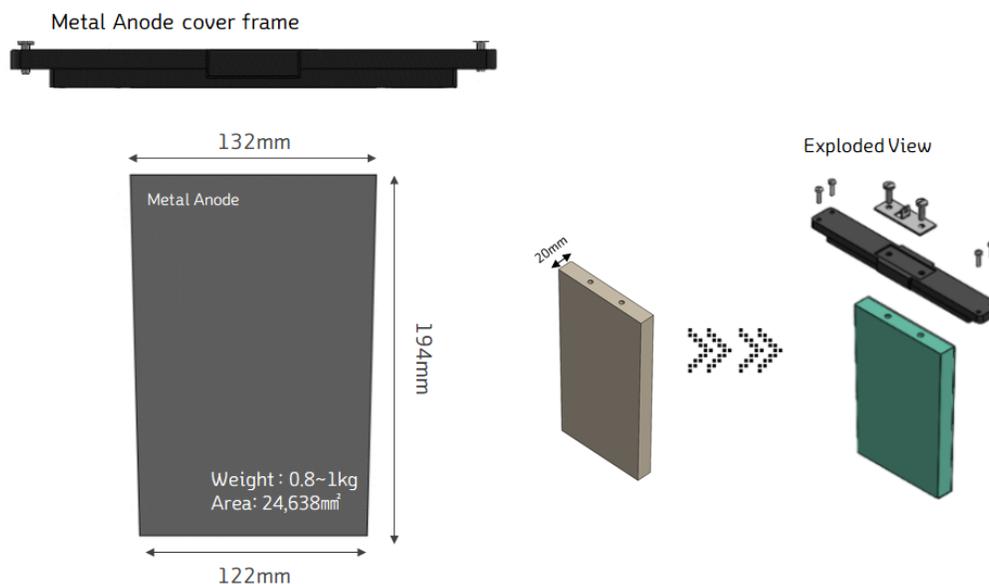
2.3. Size Selection of Mg Anode

In designing an Mg-Air Battery Cell, the first consideration is the capacity that each cell can generate. To achieve this, the size of the metal anode is the starting point. Equation (8) provides the formula for calculating the electrochemical power capacity of the Mg-anode per kilogram. Using magnesium's (Mg) standard atomic weight of 24.3 and Faraday's law of electrolysis, which involves 96,485C/mol, and the open-circuit voltage of the Mg-Air Battery at 1.2V, the theoretical power capacity of 2.2kWh per kilogram of Mg anode was derived.

In this study, to design a cell with a 2kWh capacity, the Mg anode weight was set between 0.8kg and 1kg. Based on this, cells were designed to generate between 2 and 2.2kWh of power per cell, optimizing the anode size to achieve the desired output.

$$Power\ Capacity\ (kWh) = \frac{kg}{g/mol} \times \frac{A}{mol \cdot sec} \times \frac{hr}{sec} \times MAB\ Voltage \qquad (8)$$

$$= \frac{kg}{Atomic\ Weight\ of\ Mg} \times C \times \frac{hr}{sec} \times V$$

Figure 6 illustrates the design of the metal anode in terms of its shape and size. To optimize production costs and processes, the Mg anode was designed in a trapezoidal shape. The dimensions are as follows: top length of 132mm, bottom length of 122mm, height of 194mm, and a thickness of 20t, with a total weight of 0.8kg.

This design was chosen because it allows for an economical production process using a casting method. The trapezoidal shape can be made by casting the Mg anode as an ingot and cutting it to the required thickness. This approach ensures cost-effectiveness while maintaining the necessary anode size for the desired energy output.

Figure 6. Design of Mg anode shape and size**.**

2.4. Fabrication of Air Cathode

The air cathode, a critical component of metal-air batteries, plays a crucial role in both the electrical performance and the durability of the cell. Several factors affect the lifespan of the cathode material, one of which is the accumulation of heat in the cathode's current collector due to the exothermic reactions in the metal-air battery cell. This heat buildup can lead to the collapse of the cathode's network structure. Additionally, condensation forming on the nickel current collector causes the oxidation of nickel, which further reduces the lifespan of the air cathode.

A significant cause of the cathode's degradation is the collapse of the Polymer-Carbon-Nickel (PCN) composite cathode's network structure due to condensation. This collapse leads to cracking and leakage within the cathode. Moreover, during the discharge of the MAB, byproducts (slurry) from the metal-anode reaction can attach to and accumulate on the surface of the air cathode. This buildup can cause portions of the carbon in the cathode to break off along with the byproducts, leading to further cracking and structural damage.

The conventional method of producing 300 x 300mm air cathodes using hot pressing requires substantial equipment costs. To address this, an alternative production method is proposed: using sintering, a heat treatment technique like annealing, which is more cost-effective and suitable for mass production. This approach aims to design and manufacture air cathodes that maintain performance while reducing production costs and enabling scalability.

The air cathode in this study consists of a PCN (Polymer + Carbon-based powder + Nickel) layer, and a new fabrication method was developed to enhance durability and performance. Unlike the conventional hot press method, this study utilized a rolling and heating process at atmospheric pressure to manufacture the air cathode. As shown in Figure 7, this new approach eliminates the need for specialized equipment for producing air cathodes of desired sizes, as it can be done using standard rolling mills and ovens, leading to reduced production costs.

The fabrication process follows six steps for the air cathode:
1. Material composition selection
2. Weighing the materials
3. Material mixing
4. Stirring
5. Rolling
6. Heat treatment

Detailed Fabrication Process:

1. Material Mixing: A mixture of activated carbon and cobalt oxide (Co_3O_4) in a 4:2 ratio is prepared in a mixer with a small amount of ethanol added. To ensure the materials are fully homogenized, ultrasonic treatment is applied.

2. Paste Formation: Polytetrafluoroethylene (PTFE) is gradually added to the activated carbon-Co_3O_4 mixture, and the combined mixture (wt. ratio 4:2:6) is heated to 80°C while being stirred at 300 rpm until a paste-like consistency is achieved.

3. Rolling Process: Once the mixing and heating are complete, the carbon polymer paste is fed into a rolling mill and rolled into a 0.3mm sheet. Nickel foam, which will be used as the electrode, is also rolled to a 0.3mm thickness.

4. Layering and Rolling: The carbon polymer layer in Figure 8(a) is layered onto the nickel foam, and the combined structure is passed through the rolling mill again to ensure proper bonding.

5. Heat Treatment: The rolled composite (Carbon Polymer layer + Nickel foam) is placed in an oven set to 360°C for 30 minutes to create a porous structure. This step completes the fabrication of the air cathode.

This new process not only improves the durability and performance of the air cathode but also simplifies production by using readily available equipment, making it more cost-effective and scalable.

In this study, the performance of the air cathode was compared by varying the rolling pressures of 3 tons, 10 tons, and 20 tons. After analyzing the results, the air cathode fabricated under the optimal pressure was selected and used for further research. This approach allowed for identifying the ideal rolling pressure that enhances the structural integrity, durability, and performance of the air cathode, ensuring the best possible outcome for its application in metal-air batteries.
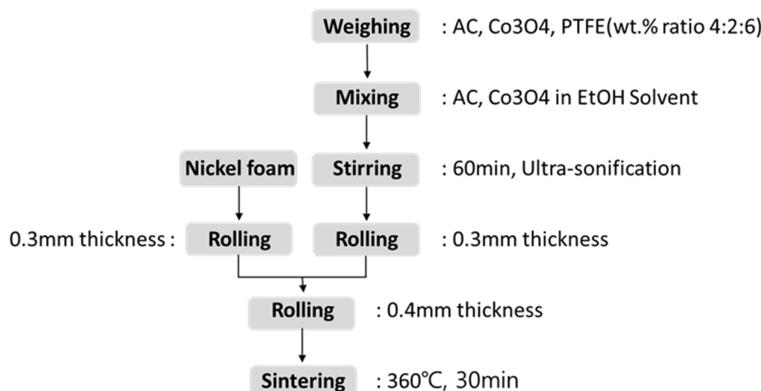
Figure 7. Manufacturing process of air cathode.

Figure 9 shows the comparison of the air cathode surface after being heated at 330°C and 360°C, observed under an optical microscope, to optimize the sintering of PTFE. Since the melting point of PTFE is 327°C, the air cathode was heat-treated at both 330°C and 360°C. To optimize the sintering of PTFE, the air cathode was heated at 330°C and 360°C, and the surface was compared using optical microscopy. Since PTFE has a melting point of 327°C, the air cathode was heat-treated at both 330°C and 360°C.

In Figure 9, images (a) and (b) display no evidence of a porous structure, confirming that the heat treatment at 330°C was insufficient for generating the desired porosity.   Conversely, images (c) and (d) show the formation of a porous structure, which indicates successful sintering at 360°C. images (a) and (b) display no evidence of a porous structure, confirming that the heat treatment at 330°C was insufficient for generating the desired porosity. This demonstrates that a higher temperature of 360°C is more effective in promoting the formation of the necessary porous network for the air cathode.
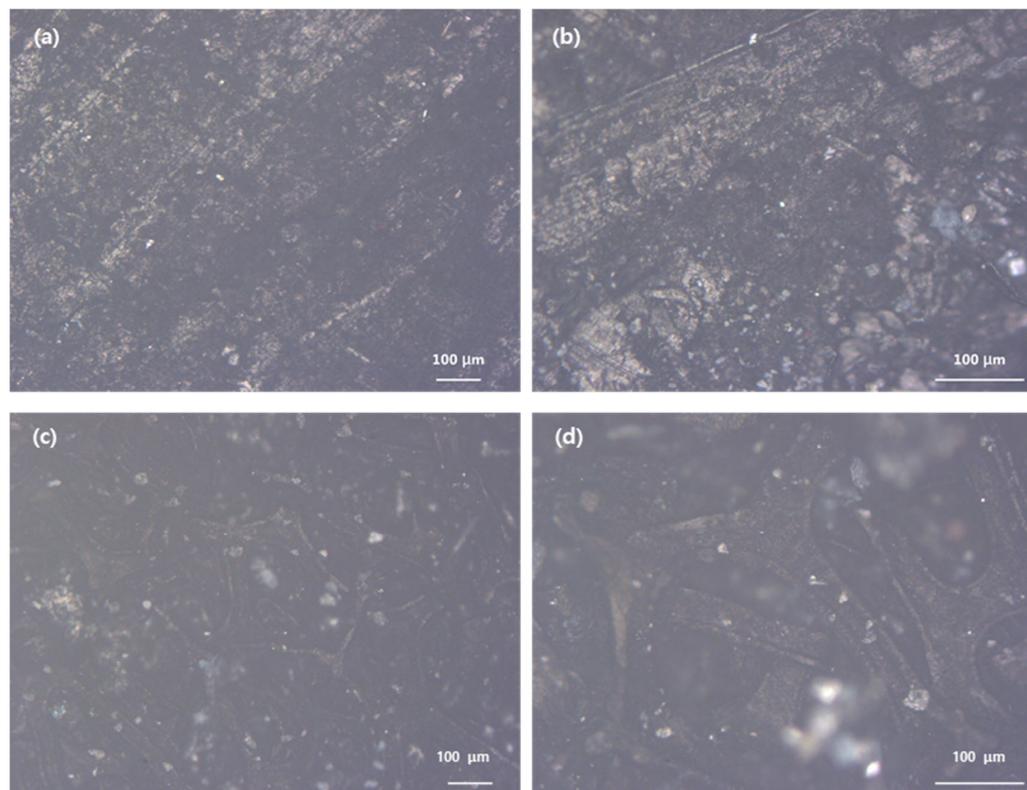
(a) Stirring and heating

(b) Rolling processing

(c) Optimally manufactured air-cathode

Figure 8. Manufacturing procedure of air cathode (a) material mixing and paste formation (b) layering and rolling process (c) optimized air cathode components after heat treatment.


Figure 9. Air cathode surface optical microscope (a), (b): 330℃, 0.5 hour (c), (d): 360℃, 0.5 hour.

Figure 10 compares the electrical energy generation performance of MAB Cells using air cathodes produced with rolling pressures of 3 tons, 10 tons, and 20 tons. The air cathode sample rolled with 3 tons of pressure exhibited the lowest performance, generating only 0.35V under a 2A

discharge condition. In contrast, the air cathode produced with 20 tons of rolling pressure demonstrated the best voltage output performance.

Additionally, the performance of the air cathode made with 20 tons of pressure was comparable to those produced by company A(MEET Co., Ltd.) and company B(IONS LAB CO., Ltd.) using hot press methods. This confirms that the air cathode fabricated with 20 tons of rolling pressure is suitable for use in the study. Therefore, the air cathode produced at 20 tons of pressure will be used in further research.
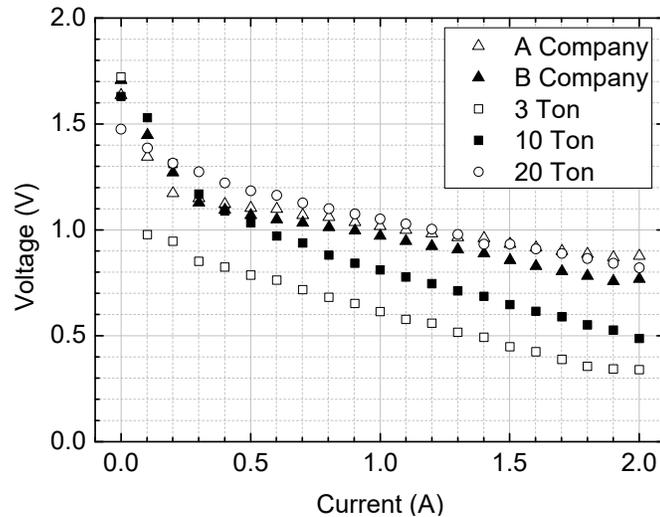
Figure 10. Comparison on electrical performance of MAB cell with various of manufactured air cathodes.

2.5. MAB Cell Frame Design for Electrical and Mechanical Optimization

Figure 11 illustrates the internal schematic of the metal-air battery cell. The overall dimensions of the cell are 265mm in height, 240mm in width, and 50mm in thickness. Polypropylene (PP) was chosen as the material for the cell's construction due to its durability and chemical resistance.
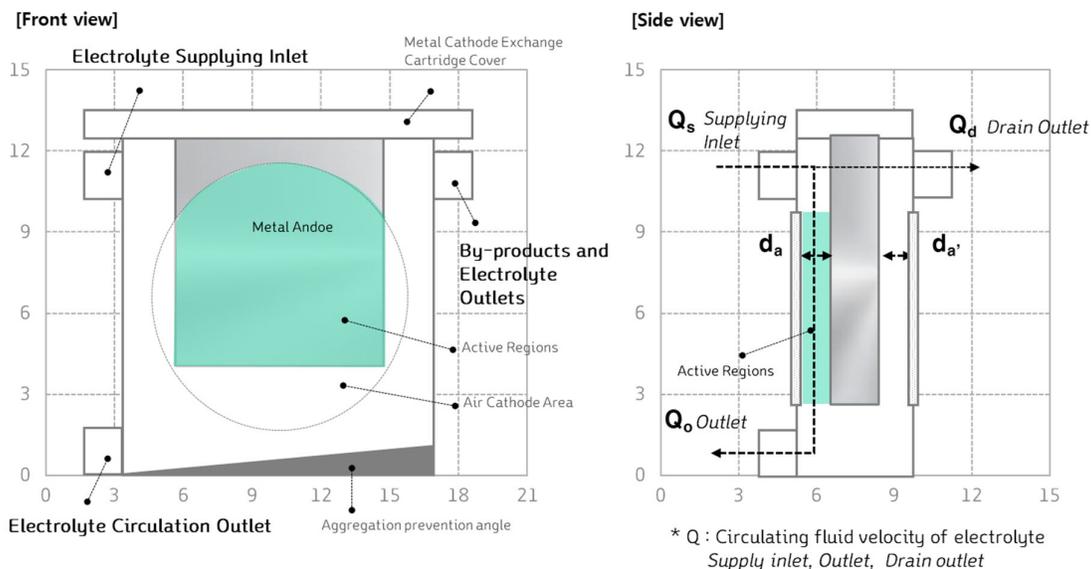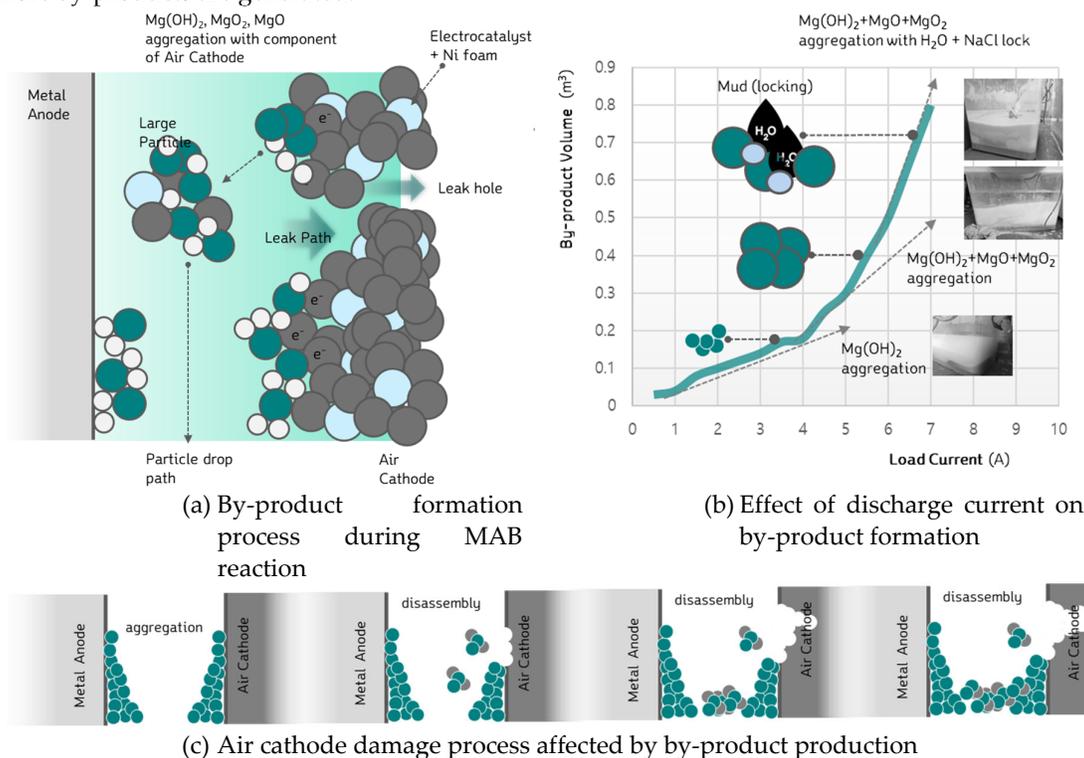
Figure 11. Internal schematic diagram of MAB cell.

To ensure the secure fixation of the air cathode and prevent electrolyte leakage, a 6Φ rubber O-ring was applied. Additionally, for strong and uniform sealing, a rotary coupling mechanism was designed for the cell cover. The cover incorporates screw threads on the inside of the circular lid,

allowing the metal-air battery cell to be tightly sealed and ensuring robust assembly. This design enhances the overall integrity and reliability of the cell during operation.

Figure 12 provides a schematic representation of byproduct formation during metal-air battery discharge. This schematic illustrates how byproducts are produced and how they accumulate within the cell, particularly focusing on the anode surface and the bottom of the cell. As shown in Figure 12 (c), this accumulation can affect the cell's performance and lifespan if not properly managed.

During metal-air battery discharge, the movement of cations and anions in the active region results in the generation of byproducts while producing electricity. As the Mg anode undergoes oxidation, byproducts such as magnesium hydroxide ($Mg(OH)_2$) and magnesium oxide (MgO) are formed. Figure 12 (a) indicates that these byproducts tend to accumulate with high density at the bottom of the cell and on the surface of the anode. Figure 12 (b) presents the effect of discharge current on by-product generation during the MAB reaction. It shows that as the discharge current increases, more by-products are generated.

(a) By-product formation process during MAB reaction

(b) Effect of discharge current on by-product formation

(c) Air cathode damage process affected by by-product production

**Figure 12.** Schematic diagram of by-products accumulating inside MAB cell.

When excessive byproducts accumulate in the metal-air battery, they can hinder power generation and, in the long term, affect the electrolyte's quality and the cell's durability. To address this issue, the cell was designed with a system that allows for the circulation and management of the electrolyte and byproducts. A drain line was added at the top of the cell to prevent over-supply of the electrolyte inside the cell.

Additionally, as shown in Figure 13, the bottom of the cell was designed with a sloped structure, making it easier for the byproducts to exit through a designated outlet. This sloped design facilitates the removal of byproducts, helping to maintain cell performance over time.

Figure 14 illustrates the schematic of the electrolyte circulation process. This system ensures that both the electrolyte and the byproducts are managed efficiently, enhancing the cell's long-term operation and preventing the detrimental effects of byproduct accumulation.
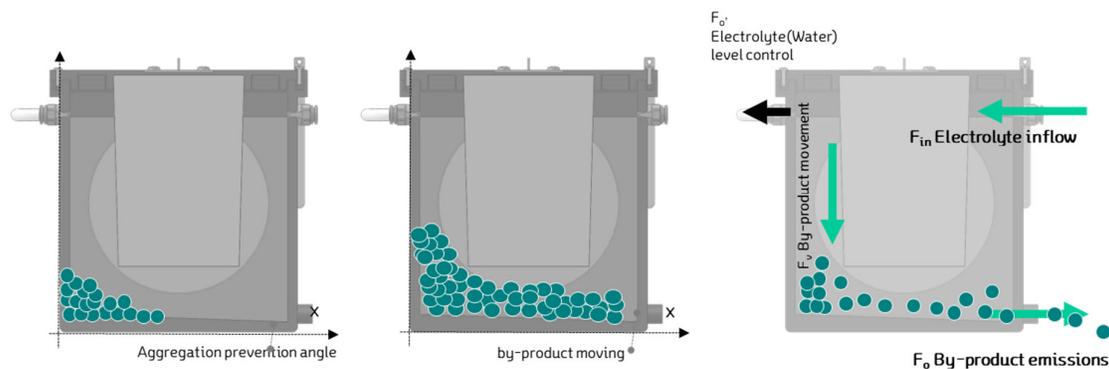
Figure 13. Electrolyte circulation process of MAB by-products and electrolyte supply and discharge inside the cell through precipitation.
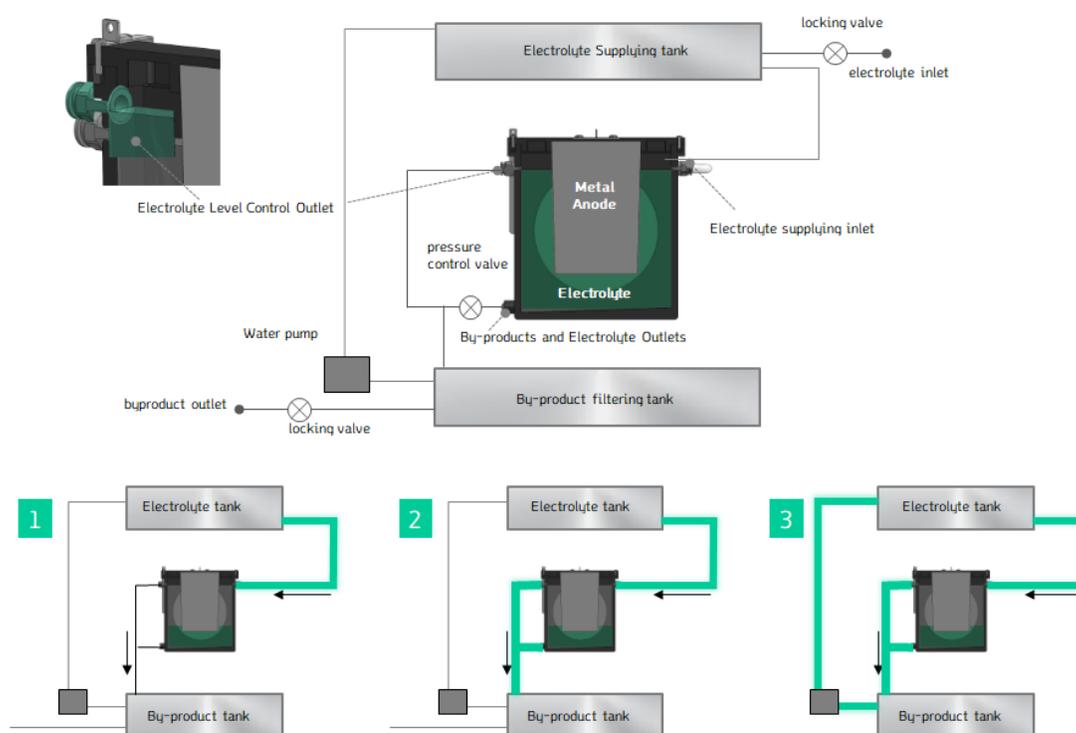
Figure 14. Schematic diagram on MAB cell electrolyte supply and discharge.

To allow easy replacement of the Mg anode in the MAB cell, a new cover design was created, enabling the Mg to be swapped out and reused. The cover is specifically designed to maintain the optimal gap distance between the Mg anode and the air cathode for the best power generation performance. The cover was designed to securely hold the Mg anode in place and allow for convenient replacement when the Mg is consumed. As shown in Figure 15, the Mg anode was designed in a cartridge format, allowing easy installation. To secure the anode, an M6-sized bolt was incorporated, with screw threads added to the anode so that it can be tightly fastened to the anode-fixing cover.

This design ensures that the Mg anode can be easily swapped out when depleted and replaced with a new one, extending the usability of the MAB cell and ensuring consistent performance.
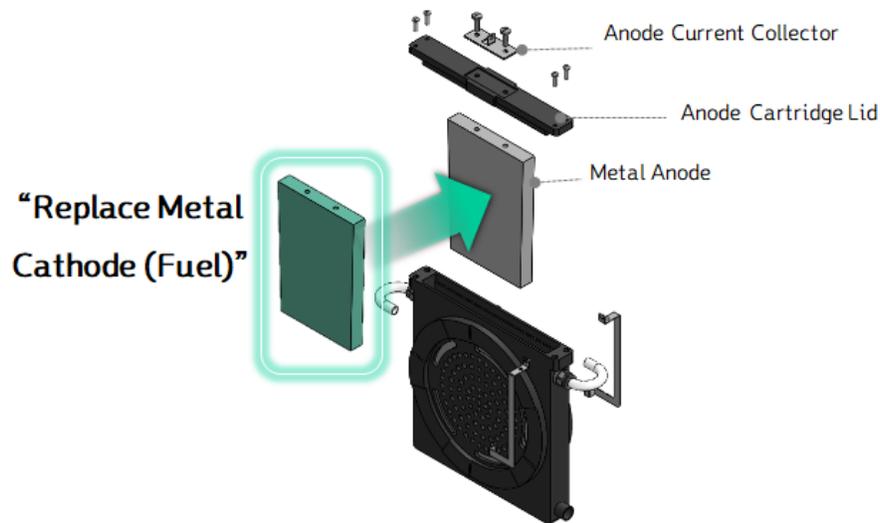
Figure 15. Disassembled/assembled diagram of MAB cell with Mg anode.

3. Results

3.1. Electrolyte-Circulation Management System (ECMS)

The electrolyte circulation system is a critical factor for maintaining the performance of the metal-air batter. For long-term use, the metal-air battery cell needs to be continuously supplied with electrolyte, and byproducts generated during power generation must be filtered to maintain performance. To assess the impact of the electrolyte circulation system on the cell, a simulation was conducted to predict how the system would affect the metal-air battery cell by analyzing the pressure applied and the fluid movement inside the cell during electrolyte supply and discharge.

The simulation was performed using SolidWorks flow simulation, with water from the SolidWorks library used as a substitute for the electrolyte. In Figure 16, the fluid flow was simulated by injecting electrolyte through the upper inlet of the metal-air battery cell and allowing it to exit through the lower outlet. The objective was to visualize and analyze the fluid dynamics inside the cell and ensure that byproducts generated during discharge could be effectively removed. As shown in Figure 17, the simulation results indicated that when injecting electrolyte at a flow rate of 28 to 122 ml/s, the electrolyte circulation within the cell was sufficient to facilitate the removal of byproducts during metal-air battery discharge. This confirmed the feasibility of the electrolyte circulation system in maintaining the cell's performance over extended use by ensuring continuous byproduct filtration and electrolyte supply.
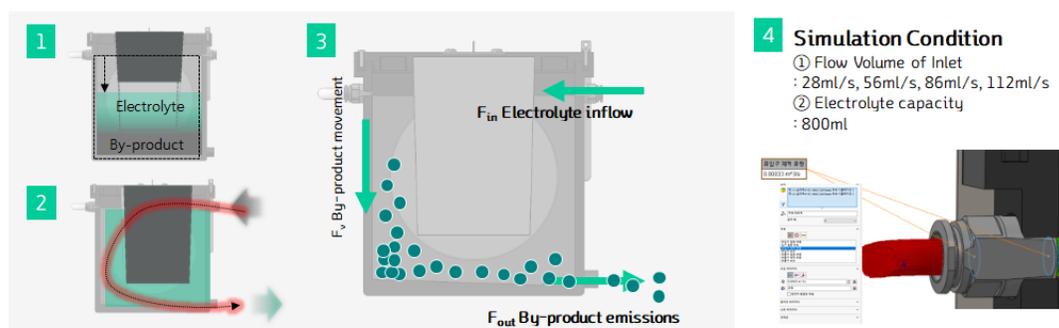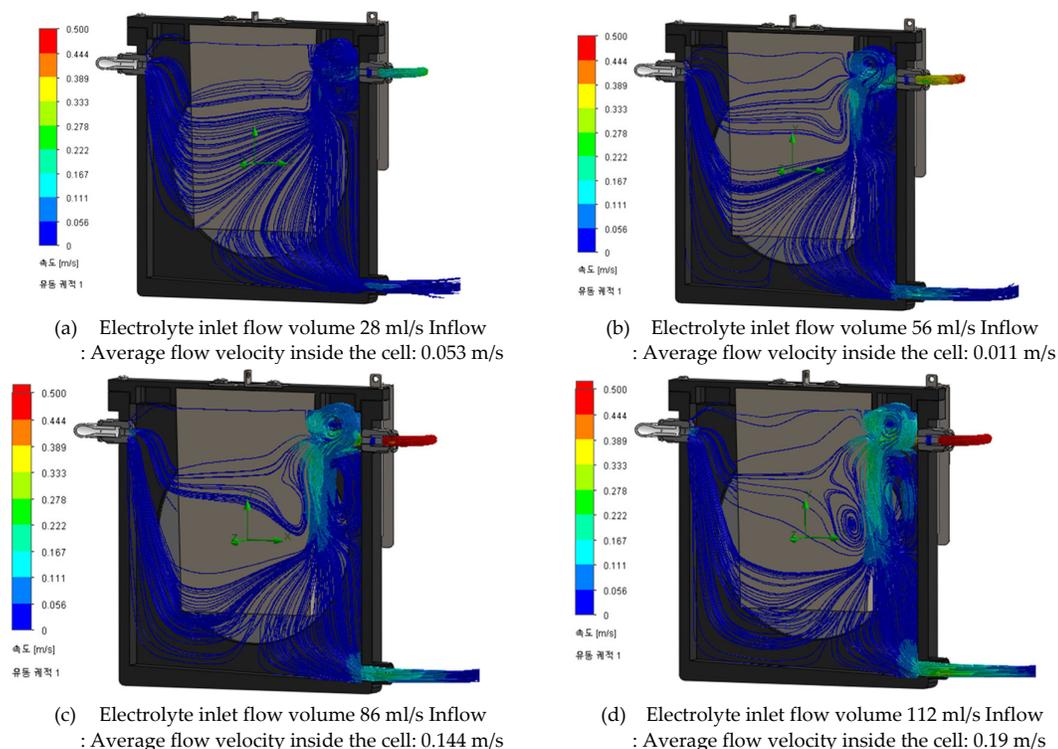

Figure 16. Electrolyte circulation simulation settings of MAB cell.

(a)   Electrolyte inlet flow volume 28 ml/s Inflow
: Average flow velocity inside the cell: 0.053 m/s

(b)   Electrolyte inlet flow volume 56 ml/s Inflow
: Average flow velocity inside the cell: 0.011 m/s

(c)   Electrolyte inlet flow volume 86 ml/s Inflow
: Average flow velocity inside the cell: 0.144 m/s

(d)   Electrolyte inlet flow volume 112 ml/s Inflow
: Average flow velocity inside the cell: 0.19 m/s

Figure 17. Electrolyte Cycle Simulation of MAG cell.

3.2. Electrical Performance of Mg-Air Battery

Figure 18 shows the experimental setups for the discharge test of Mg-Air Battery(MAB) cell. The electrical performance of the final designed MAB Cell is a critical aspect. Figure 19 presents the voltage graph corresponding to changes in discharge current, ranging from 1A to 8A. The discharge current was increased by increments of 0.5A, and the voltage was measured over a period of 300 seconds for each current level.
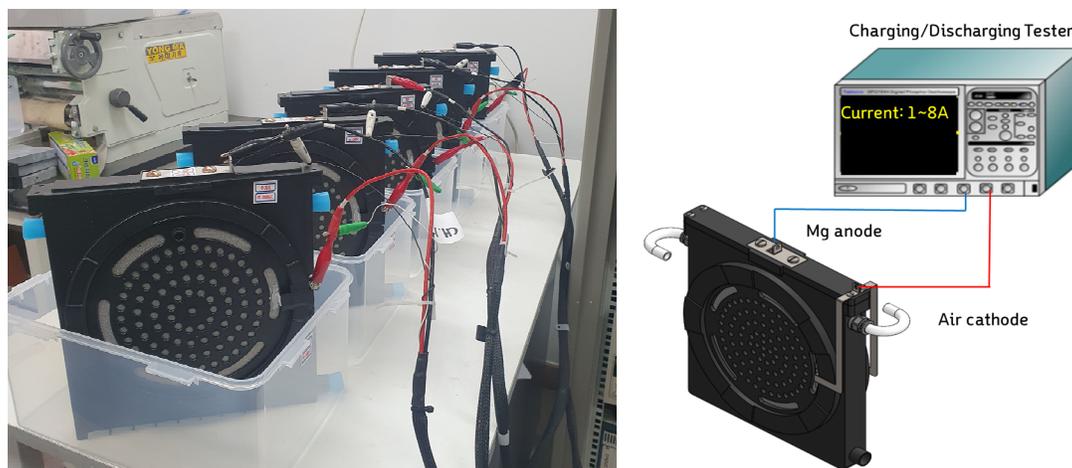
Figure 18. Discharge test of MAG unit cell.

The results in Figure 20 indicate a significant voltage drop beyond 7.5A, showing a steep decline in performance at higher currents. The maximum power point was observed to occur between 7.0A and 7.5A. This suggests that while the MAB cell can handle higher currents, its optimal performance is achieved just before the sharp voltage drop at 7.5A. This data is crucial for understanding the operational limits and efficiency of the MAB cell under different load conditions.
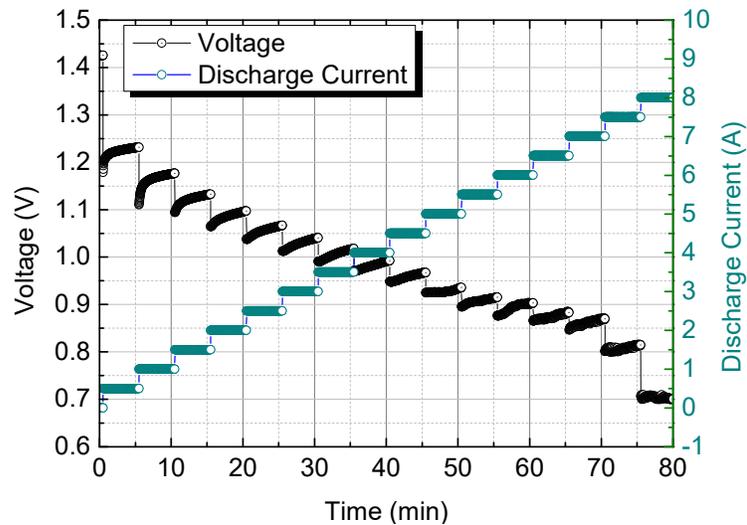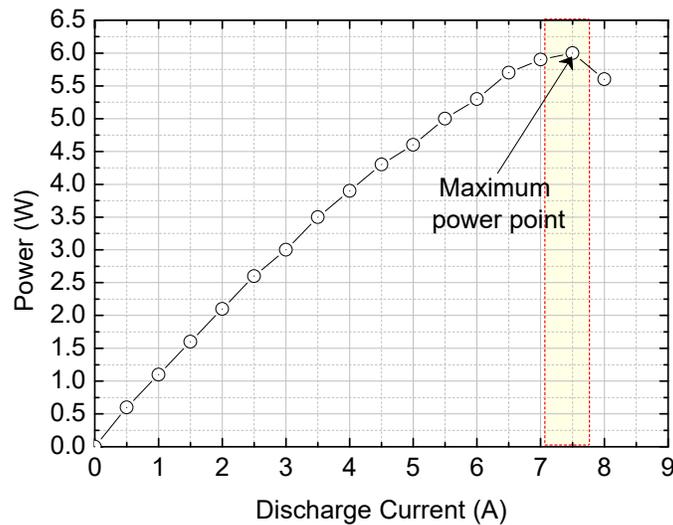
Figure 19. I-V curve of MAB cell.

Figure 20. Power optimization of MAB cell.

4. Conclusions

Recent research on metal-air batteries has primarily focused on improving lifespan and electrical performance by reducing metal corrosion through the use of metal alloys. There has also been an emphasis on designing small cells for mobility and portable electronic devices. In contrast, this study focused on developing metal-air battery designs and performance evaluations aimed at distributed power generation technologies based on eco-friendly energy sources, with the goal of reducing carbon emissions. Specifically, the study aimed to design large-capacity Mg-Air Battery(MAB) cells for Metal-Air Generators (MAG) suitable for off-grid environments. To achieve the optimal MAB cell design, the performance characteristics of the metal anode were analyzed. The electrical performance of five different types of commercial Mg alloys (Pure Mg, LZ41, AL41, ZK60, and AZ31) was compared, and the most suitable Mg alloy material was selected. Experiments were conducted to determine the allowable gap distance between the metal anode and air cathode (ranging from 0.5mm to 4.5mm), ensuring optimal cell design. The air cathode was manufactured using a rolling process, and its performance was evaluated under different applied pressures.

Various factors influencing the performance of the Mg anode and air cathode were examined to design the MAB cell, which was finalized with dimensions of 265mm in height, 240mm in width, and

50mm in thickness. To ensure long-term performance, an electrolyte supply and circulation system was implemented, and SolidWorks flow simulation was used to confirm the internal circulation of the cell based on the electrolyte supply flow rate.

Electrical performance was assessed by measuring the voltage output at discharge currents ranging from 0A to 8A, increasing in 0.5A increments. The maximum power performance was observed at a discharge current of 7.5A. Finally, the study confirmed the feasibility of creating a large-capacity MAG system for off-grid power supply by combining multiple MAB cells in series and parallel to achieve a kilowatt-scale system.

References

1. Wang, F.; Harindintwali, J.D.; Yuan Z.; et al. Technologies and perspectives for achieving carbon neutrality, *The Innovation*, **2021**, 2
2. Chen J.M. Carbon neutrality: Toward a sustainable future, *The Innovation*, **2021**, 2, 100180
3. Rabaey, K.; Ragauskas A.J; Editorial overview: Energy Biotechnology, *Current Opinion in Biotechnology*, **2014**, 27, 5-6
4. Mora, C.; Spirandelli, D. et al. Broad threat to humanity from cumulative climate hazards intensified by greenhouse gas emissions, *Nature Climate Change*, **2018**, 8, 1062–1071
5. Yang, M.; Chen, L.; Msigwa, G.; Tang, K.H.D; Yap, P.S. Implications of COVID-19 on global environmental pollution and carbon emissions with strategies for sustainability in the COVID-19 era, *Science of The Total Environment*, **2022**, 809, 151657.
6. Yaqoob, L.; Noor,T.; Iqbal, N. An overview of metal-air batteries, current progress, and future perspectives, *Journal of Energy Storage*, **2022**, 56, 106075
7. Uimonen, T. Mathematical Modelling of Metal-Air Battery, University of Vaasa, **2018**
8. Poonam, Bhatnagar, J.K.; Sharma, R.C. A Review of Magnesium Air Battery Systems: From Design Aspects to Performance Characteristics, *International Journal of Material Science and Engineering*, **2021**, 7, 18-28
9. Wang, Y.; Sun, Y.; Ren, W.; Zhang, D.; Yang, Y.; Yang, J.; Wang, J.; Zeng, X.; NuLi,Y. Challenges and prospects of Mg-air batteries: a review, *Energy Materials,* **2022**, 2, 200024
10. Zhang, T.; Tao, Z.; Chen, J. Magnesium–air batteries: from principle to application, *Materials Horizons*, **2014**, 1, 196–206
11. Wang, N.; Huang, Y.; Liu, J; Yang, X.; Xie, W.; Cai, Q.; Zheng, S.; Shi, Z. AZ31 magnesium alloy with ultrafine grains as the anode for Mg-air battery, *Electrochimica Acta*, **2021**, 378, 138135
12. Chen, X.; Wang,H.; Zou, O.; Le, O.; Wen, C.; Atrens, A. The influence of heat treatment on discharge and electrochemical properties of Mg-Gd-Zn magnesium anode with long period stacking ordered structure for Mg-air battery, *Electrochimica Acta,* **2021**, 367, 137518
13. Wang, N.; Wang, R.; Peng, C.; Peng,B.; Feng, Y.; Hu, C. Discharge behaviour of Mg-Al-Pb and Mg-Al-Pb-In alloys as anodes for Mg-air battery, *Electrochimica Acta*, **2014**, 149, 193-205
14. Peng, B.; Liang, J.; Taoa, Z.; Chen, J. Magnesium nanostructures for energy storage and conversion, *Journal of Materials Chemistry*, **2019**, 19, 2877-2883
15. Liu, R.L.; Scully, J.R.; Williams, G.; Birbilis, N. Reducing the corrosion rate of magnesium via microalloying additions of group 14 and 15 elements, *Electrochimica Acta*, **2018**, 260, 184-195
16. Huang, X.; Dai, O.; Xiang, Q.; Yang, N.; Zhang, G.; Shen, A.; Li, W. Microstructure design of advanced magnesium-air battery anodes, *Journal of Magnesium and Alloys*, **2024**, 12, 443-464
17. Le, T.; Mao, P.; Hu, W.; Le, O. The electrochemical corrosion behaviors and Mg-air battery anode performance of Mg–1Sn–1Ca-0.3Mn alloy with different grain size and Mg2Ca morphology, *Journal of Power Sources*, **2024**, 608, 234297
18. Wei, C.; Tan, L.; Zhang, Y.; Wang, Z.; Feng, J.; Qian, Y. Towards better Mg metal anodes in rechargeable Mg batteries Challenges, strategies, and perspectives, *Energy Storage Materials*, **2022**, 52, 299-319
19. Alemu, M, A. Worku, A.K.; Getie, M.Z. Recent advancement of electrically rechargeable alkaline Metal-Air batteries for future mobility, *Results in Chemistry*, **2023**, 6, 101048
20. Tong, F.; Chen, X.; Wang, Q.; Wei, S.; Gao, W. Hypoeutectic Mg–Zn binary alloys as anode materials for magnesium-air batteries, *Journal of Alloys and Compounds*, **2021**, 857, 157579
21. Zhuk, A.; Belyaev, G.; Borodina, T.; Kiseleva, E.; Shkolnikov, E.; Tuganov, V.; Valiano, G.; Zakharov,V. Magnesium–Air Battery with Increased Power Using Commercial Alloy Anodes, *Energies*, **2024**, 17
22. Tong, F.; Wei, S.; Chen, X.; Gao, W. Magnesium alloys as anodes for neutral aqueous magnesium-air batteries, *Journal of Magnesium and Alloys*, **2021**, 9, 1861-1883
23. Zhao, Y.; Huang, G.; Wang, G.; Yao, Z.; Peng, C.; Pan, F. Corrosion and Discharge Performance of Mg-2Zn-0.5Ce-0.5Mn- 0.2Ca Alloy in NaCl Solution, *International Journal of Electrochemical Science*, **2020**, 15, 1082-1090

24. Shi, Y.; Peng, C.; Feng, Y.; Wang, R.; Wang, N. Microstructure and electrochemical corrosion behavior of extruded Mg–Al–Pb–La alloy as anode for seawater-activated battery, *Materials & Design*, **2017**, 124, 24-33

25. Chen, Z.; Zhang, Y.; Ma, M.; Zhang, K.; Li, Y.; Shi, G.; Yuan, J.; Sun, Z.; Zhao, G. The discharge and corrosion performances of as-cast Mg-Ga-Sn anodes for the primary magnesium-air battery, *Materials Chemistry and Physics*, **2023**, 300, 127500

26. Liu, X.; Xue, J.; Liu, S. Discharge and corrosion behaviors of the α-Mg and β-Li based Mg alloys for Mg-air batteries at different current densities, *Materials & Design*, **2018,** 160, 138-146

27. Liu, X.; Xue, J.; Zhang, P.; Wang, Z. Effects of the combinative Ca, Sm and La additions on the electrochemical behaviors and discharge performance of the as-extruded AZ91 anodes for Mg-air batteries, *Journal of Power Sources*, **2019**, 414, 174-182

28. Deng, M.; Höche, D.; Lamaka, S.V.; Snihirova, D.; Zheludkevich, M.L. Mg-Ca binary alloys as anodes for primary Mg-air batteries, *Journal of Power Sources*, **2018**, 396, 109-118

29. Sivashanmugam, A.; Kumar, T.P.; Renganathan, N. G.; Gopukumar, S. Performance of a magnesium–lithium alloy as an anode for magnesium batteries, *Journal of Applied Electrochemistry*, **2004** 34, 1135-1139

30. Wu, Z.; Zhang, H.; Qin, K.; Zou, J.; Qin, K.; Ban, C.; Cui, J.; Nagaumi, H. The role of gallium and indium in improving the electrochemical characteristics of Al–Mg–Sn-based alloy for Al–air battery anodes in 2M NaCl solution, *Journal of Materials Science*, **2020**, 55, 11545-11560